

Fermi National Accelerator Laboratory

FERMILAB-Pub-86 / 147-T

November 7, 1986

Ultra-High Energy Cosmic Rays From Superconducting Cosmic Strings

Christopher T. Hill

Fermi National Accelerator Laboratory

P.O. Box 500

Batavia, Ill. 60510

David N. Schramm

Fermilab Astrophysics Group and

University of Chicago

Chicago, Ill., 60637

Terry P. Walker

Department of Physics

Boston University

Boston, Massachusetts, 02215

Abstract

Superconducting cosmic strings may play an important role in the relatively late Universe in formation of structure and in driving highly exoergic processes. With fermionic charge carriers they are expected to eject, in their last stages, high mass particles which can subsequently decay to produce ultra-high energy electromagnetic, neutrino and hadronic radiation. Cosmic ray physics places significant limits on these scenarios. We find, for example, that the fermion mass must be substantially smaller, $\leq 10^{13}$ Gev, than the presumed scale of the broken $U(1)$. This provides a mechanism for the production of the observed ultra-high energy cosmic rays with some characteristically unusual features.



I. Introduction

Recently Ostriker, Thompson, and Witten [1] (hereafter denoted OTW) proposed a dramatic scenario for a highly exoergic late Universe involving the decay of cosmic flux tubes which have superconducting electromagnetic boundary conditions. That such objects might exist in certain grand unified theories (GUTs) was first proposed by Witten [2]. Superconducting cosmic strings rely either upon the existence of superheavy fermions (which have ordinary electric charge and receive a pairing mass from the Higgs associated with the breaking of an extra $U(1)$ symmetry and which can become trapped as Jackiw-Rossi zero modes on the string), or upon a bosonic construction which we shall not directly consider in the present paper (some of the estimates will have analogues in the bosonic case). In the fermionic case, massless Jackiw-Rossi zero modes act as carriers of electromagnetic currents and the flux tube becomes superconducting. Thus if one has a closed loop with a primordial threading magnetic field, pairs of zero modes are created on the string as the magnetic field is withdrawn and constitute the induced current. The OTW scenario presupposes the existence of primordial magnetic fields to set up this current.

Once electromagnetic currents are achieved and in the extreme relativistic limit of the string, electromagnetic quadrupole radiation is produced which can drive various effects which may be of importance to form galaxies and large scale structure in the Universe and accelerate the relaxation of the string. As the loop shrinks the trapped fermion zero-modes eventually become degenerate. The upper limit on the fermi-energy is given by the vacuum expectation value (VEV) of the Higgs which breaks the extra $U(1)$. Above this energy fermions cease to be trapped on the string and will be ejected into the vacuum.

In the vacuum away from the string the fermions presumably act as superheavy (GUT mass) particles and are expected to decay, probably into 3 body final states involving conventional quarks and leptons, or into 2-body states with a conventional fermion and some gauge boson or Higgs. This leads to : (i) direct neutrinos, (ii) direct electrons and gammas, and (iii) quarks which fragment into hadrons leading to: (iii.a) protons, (iii.b)neutrons, (iii.c) neutrinos, and (iii.d) electrons and gammas. At an earthbound detector one records a highly *evolved* spectrum via: (a) redshift of the injection spectrum, (b) energy loss and recoil pile-up due to

collisions with microwave photons (ambient dust, starlight and ordinary matter are generally negligibly smaller effects), source debris, and in-source magnetic fields, and (c) produced secondaries such as neutrinos and electrons and gammas by pion photoproduction in the above collisions. We emphasize that neutrons comprise 50% of the surviving hadronic component because at these energies they can live for > 10 Mpc and lose no energy due to Larmor radiation in the source. We do not concern ourselves with the electromagnetic component which involves a more complex evolution study and is more than likely reduced to a degraded thermal spectrum due to the intense B-fields in the vicinity of the saturated string (for a discussion see ref.[3]).

In this paper, we examine the dynamics of superconducting loops and consider the evolution of the hypothetical unstable fermion pairs they emit. First we show that such loops cannot be supported by the degeneracy pressure of fermion zero-modes, assuming a perturbative GUT. We then suppose the standard string loop formation distributions and gravitational energy loss as embodied in usual cosmic string scenarios[4] and, along with very general assumptions about the magnetic field history of loops responsible for establishing the currents, we calculate the density of fermion emitting loops as a function of redshift.

By modeling the fragmentation distribution function of the quarks in a manner consistent with QCD multiplicity expectations and evolving the resultant hadrons thru the background radiation, we predict the ultra-high energy hadronic cosmic ray spectrum associated with the superconducting loops. The dominant neutrino spectrum is directly obtained from the decays of massive fermions and from pions produced in quark fragmentation. (We can safely neglect the induced neutrino spectrum resulting from the transport of the nucleons through the microwave background as shown below, though results obtained previously [5, 6] are readily adaptable). We find that these scenarios are severely constrained by such limits as the Fly's Eye data on deeply penetrating particles with energies $> 10^{17}$ *ev*. Respecting such limits we find that it is plausible to generate the observed ultra-high energy cosmic rays via the decays of superheavy fermions emitted by saturated superconducting strings.

II. Evolution of the Superconducting String

A. Do Flux Tubes Have a Chandrasekhar Limit?

One important issue is the approach to the extremely degenerate situation in which the string is no longer described by the worldsheet area action. It becomes of interest to see if the loop can be stabilized by fermion degeneracy, i.e. develop a Chandrasekhar limit. Within the assumption of perturbativity we find this does not occur.

We may consider an effective potential for a string of length L :

$$E \approx \frac{v^2 L}{\alpha'} + \frac{\pi N^2}{L} \quad L > L_s \quad (2.1)$$

where v is the Higgs VEV which breaks the $U(1)$ associated with the flux tube, N the number of fermions of a given chirality plus antifermions of the opposite chirality (thus N has a positive or negative sign associated with the sense of the current and the current is $2eN/L$), L_s is the string length at saturation, and we neglect the energy associated with the self-interaction of the fermions. Here α' is the broken $U(1)'$ coupling (squared over 4π) at the scale v , which we presume throughout to be < 1 . Thus the mass per unit length, μ , is v^2/α' and for typical values expected in grand-unified theories of $v \approx 10^{15}$ Gev and $\alpha' \approx 1/40$ we have $\mu \approx 4 \times 10^{21}$ gm/cm ($G_N \mu \simeq 10^{-6}$).

The number of fermions is related to the fermi-momentum as:

$$L \int_0^{k_F} \frac{dk}{2\pi} = N = \frac{Lk_F}{2\pi} \quad E_F = |k_F| \quad (2.2)$$

and the saturation fermi-energy is given roughly by the Higgs–Yukawa coupling of the heavy fermions to the $U(1)'$ breaking Higgs:

$$E_{F_s} \approx gv \quad \text{hence} \quad L_s = \frac{2\pi N}{gv} \quad \text{and} \quad J_s = 4\pi\alpha g^2 v^2, \quad (2.3)$$

where g is the Higgs–Yukawa coupling constant, α is the fine-structure constant, and J_s the saturation current. One can simply view g as the ratio $g = M_F/v$ where M_F is the fermion mass. Since eq.(2.1) applies only above saturation we see that the minimum could only be reached if:

$$L_s^2 < \frac{\pi N^2 \alpha'}{v^2} \quad \text{or} \quad 1 < \frac{g^2 \alpha'}{4\pi} \quad (2.4)$$

Since such a large Higgs–Yukawa constant as implied by eq.(2.4) is nonperturbative, we presume that there is no stable groundstate for the flux tube given by a *Chandrasekhar limit*. This further means that the second term in eq.(2.1), which is an effective mass density on the string, is never large compared to the first. Note that we might expect $\frac{g^2 \alpha'}{4\pi}$ to be as large as 1/10 in extreme cases and of order a few percent in general.

B. Energy Loss Phases

We wish to obtain a schematic picture of the energy loss phases of the superconducting string. This is somewhat different than the pure gravitational energy loss picture of ordinary strings since, as pointed out by OTW, electromagnetic energy loss dominates gravity in the late stages of evolution. In addition, loss of fermions from the top of the Fermi distribution affects the extreme final stage. Our analysis is grossly simplified as we study the static potential of the preceding section which neglects kinetic terms.

We consider a loop of size L_f which forms at a time t_f . There may be an initial induced current J_f and thus a fermion number $N_f = J_f L_f / 2e$ (below we consider the growth of the current as a primordial flux is withdrawn). Initially the string loses energy by gravitational radiation with a power $P_g = \gamma_g G_N \mu^2$, where γ_g is a factor dependent only on the loop's shape and takes values ranging from 50-100[7]. Thus we have:

$$\gamma_g G_N \mu^2 = - \left(\mu - \frac{\pi N^2}{L^2} \right) \dot{L} + \frac{2\pi N \dot{N}}{L} \quad (2.5)$$

and as we are far from degeneracy (and things are perturbative) the second and third terms on the rhs may be dropped. The string thus shrinks linearly with time:

$$L(t) \approx L_f - \kappa_1(t - t_f) \quad \kappa_1 = \gamma_g G_N \mu \quad (2.6)$$

The rate κ_1 is approximately $3 \times 10^6 \text{ cm s}^{-1}$ for $G_N \mu = 10^{-6}$ and $\gamma_g \approx 100$, values which are consistent with the cosmic string scenario of galaxy formation[7]. We

see that loops formed at $z > (1/\kappa_1)^{2/3} \approx 460 (100/\gamma_g)^{2/3} (G_N \mu/10^{-6})^{-2/3}$ will have gravitationally evaporated by today.

There will generally be a build-up of the electromagnetic current as the string shrinks due to the withdrawal of magnetic flux. The power loss in electromagnetic radiation is given by $P_e = J^2 \gamma_{em} = \gamma_{em} 16\pi \alpha N^2 / L^2$, where γ_{em} is a term analogous to γ_g (we take $\gamma_g = \gamma_{em} \approx 100$ in subsequent calculations), and eventually becomes the dominant energy loss mechanism at a scale $L_{em}^2 \leq \gamma_{em} 16\pi \alpha N^2 / (\gamma_g G_N \mu)$. In this regime the loop evolution is described by the equation:

$$\gamma_{em} \frac{16\pi \alpha N^2}{L^2} = - \left[\mu - \frac{\pi N^2}{L^2} \right] \dot{L} + \frac{2\pi N \dot{N}}{L} \quad (2.7)$$

and neglecting the fermi-energy and assuming $\dot{N} \approx 0$, the loop size is now given by:

$$L(t) = \left(L_{em}^3 - \bar{\kappa}_2 (t - t_{em}) \right)^{1/3} \quad \bar{\kappa}_2 = 48\pi \alpha N^2 \gamma_{em} / \mu \quad (2.8)$$

For comparison we define the quantity:

$$\kappa_2 = \bar{\kappa}_2 / L^2 = 12\pi \gamma_{em} \alpha \alpha' g^2 j^2 \quad (2.9)$$

where $j \equiv J/J_s$. We find that $\kappa_2 = 2.1 \times 10^{10} (g^2)(j^2) \text{ cm/sec}$. Since the OTW scenario relies upon initial values of $P_e/P_g > 10^{-4}$ (assuming $G_N \mu = 10^{-6}$) and since $j \leq 1$ we see that the *mathematical* lower limit on the fermion Higgs–Yukawa coupling is $g > 0.3 \times 10^{-4}$ and a fermion mass limit of $M_F > 0.3 \times 10^{11} \text{ Gev}$.¹

Finally the loop becomes saturated at a length of $L_s = 2\pi N_s / gv$ and continues to lose energy by emitting fermion pairs as well as electromagnetic radiation. The saturation length must be computed from a knowledge of the magnetic field history experienced by the loop (see Section II.C) The energy loss equation below the saturation length becomes:

$$\gamma_{em} \frac{4\pi \alpha N(t)^2}{L^2} = - \left[\mu - \frac{\pi N^2}{L^2} \right] \dot{L} + \frac{2\pi N \dot{N}}{L} \quad (2.10)$$

¹It should be noted that in the OTW analysis the Higgs–Yukawa coupling is implicitly taken to be of order unity. Thus they conclude that at $j \approx 10^{-2}$ the electromagnetic energy loss dominates gravitational. More generally, this occurs when $\kappa_2/\kappa_1 \approx 1$ or $gj \approx 10^{-4}$ and in most of the expressions in OTW involving j one can substitute gj .

where the last term on the rhs reflects the additional energy loss due to the creation of fermion pairs of energy E_F . Again the second and third terms can be neglected on the *rhs* of eq.(2.10). Noting that the power on the lhs of eq.(2.10) involves the ratio $N(t)^2/L(t)^2$ which is a constant when the system is saturated, we find the behavior for $L(t)$ is again linear:

$$L(t) \approx L_s - \kappa_3(t - t_s) \quad \kappa_3 = \gamma_{em} J_s^2 / \mu = 4\pi\alpha\gamma_{em}\alpha'g^2 \quad (2.11)$$

and the fermion number of the string is just:

$$N(t) = \frac{gv}{2\pi} L(t) \quad L < L_s \quad (2.12)$$

In this phase we note that the particle production rate from a saturated string relevant to the cosmic ray injection spectrum is given by:

$$\dot{N}(t) = \frac{g^2\alpha'}{2\pi} (\gamma_{em} J_{sat}^2) / M_F = 2\gamma_{em}\alpha\alpha'g^3v \quad (2.13)$$

where $M_F = gv$ is the fermion mass.

C. Magnetic Flux and Saturation

We have previously obtained the rate of particle production from a saturated string and we have sketched the time scales from formation to a given epoch at which the string becomes saturated (primarily determined by the gravitational energy loss). To proceed we require the densities of saturated strings at any redshift. This depends upon the magnetic field history experienced by the loop. We find that a simple parameterization can be given which allows a discussion of the case of OTW, with strong B-fields at large z , and more conservative cases in which known B-fields are assumed to have formed in the relatively recent past.

The number density of cosmic strings at a given epoch can be estimated from the numerical studies of Albrecht and Turok [4] who find that at a given time t , the probability of having a string with length of order the horizon size, $H(t)^{-1}$ is approximately one. More precisely, they find that there is one string formed with length

$$L_f \approx 0.87H_0^{-1}(1 + z_f)^{-3/2} \quad (2.14)$$

per horizon volume per Hubble time, where we have assumed that we are interested in the loops formed in a matter dominated $\Omega = 1$ Universe so that the scale factor evolves as $t^{2/3}$ and the current age of the Universe is just $\frac{2}{3}H_0^{-1}$ with H_0 the Hubble constant. This formation rate gives rise to a redshifted loop length distribution at later times of:

$$\frac{dn}{dL_f}(t) = \frac{0.2}{L_f^4} \left(\frac{1+z}{1+z_f} \right)^3 = 0.3H_0^2 \frac{(1+z)^3}{L_f^2} \quad (2.15)$$

where z_f and z are redshifts at t_f and t , respectively. The loops are decaying for most of their history by gravitational energy loss and we see using eq.(2.7), that loops of size $L(z)$ came from loops of size L_f given by:

$$L(z) \approx L_f - \frac{2\kappa_1}{3}H_0^{-1} \left\{ (1+z)^{-3/2} - (1+z_f)^{-3/2} \right\} \quad (2.16)$$

or

$$L_f \approx \left[L(z) + \left(\frac{2\kappa_1}{3}H_0^{-1} \right) (1+z)^{-3/2} \right]. \quad (2.17)$$

neglecting κ_1/c relative to unity. Thus we obtain the differential number density of loops with length L at any redshift:

$$\frac{dn(z)}{dL} = \frac{0.3(1+z)^3 H_0^2}{\left[L + (2\kappa_1/3)H_0^{-1}(1+z)^{-3/2} \right]^2} \quad (2.18)$$

In the equation above, $(2\kappa_1/(3H_0))(1+z)^{-3/2}$ represents the initial size of loops which have gravitationally evaporated by a redshift z and since we are always interested in small loops with size $L \ll (2\kappa_1/(3H_0))(1+z)^{-3/2}$, we see that the differential distribution of saturated loops is essentially independent of decaying loop length:

$$\frac{dn(z)}{dL} = \frac{0.6H_0^4}{\kappa_1^2} (1+z)^6 \quad (2.19)$$

Thus, if we know the saturation length from the magnetic history we have the density of saturated loops determined as:

$$n(z) = \frac{0.6H_0^4 L_s(z)}{\kappa_1^2} (1+z)^6 \quad (2.20)$$

Using the canonical value of κ_1 , eq.(2.19) represents about $2 \times 10^8 L_s H_0$ loops actively decaying within our Hubble volume today.

To calculate the saturation length as a function of redshift, we must assume a model for the magnetic field. The B-field and its correlation length $\lambda(z)$ can be parameterized as:

$$B(z) = (1+z)^{-p+3/2} B_0 \quad \lambda(z) = \lambda_0 / (1+z) \quad (2.21)$$

where $B_0 \simeq 10^{-7} \text{gauss}$ and $\lambda_0 \simeq 1 \text{ Mpc}$ are typical values for current epoch intergalactic magnetic fields as evidenced by intercluster synchrotron emission[8]. With such a parameterization, $p = -1/2$ corresponds to a primordial magnetic field energy density which scales as radiation density (as was assumed by OTW) and $p > -1/2$ would correspond to the fields generated by galactic dynamos in recent epochs.

The saturation length is determined by the history of the magnetic flux crossing the loop during its lifetime and can be parametrized as:

$$L_s \simeq \frac{\pi f(L, \lambda, z) \langle \Phi \rangle}{2egv \ln(L/2\pi l)} \quad (2.22)$$

where we include the self-inductance of a loop of thickness $l \simeq (gv)^{-1}$. Here $\langle \Phi \rangle$ is taken as the averaged flux given by

$$\langle \Phi \rangle = \frac{1}{z_f - z} \int_z^{z_f} B(z) \lambda(z)^2 dz \quad (2.23)$$

and $f(L, \lambda, z)$ is a factor accounting for \sqrt{N} fluctuations in the B-field, given roughly by L/λ for a loop of area L^2/λ^2 . We estimate that loops which produce cosmic rays observable at the current epoch will have both $f(L, \lambda, z) \approx f_\Phi$, and $\ln(L/2\pi l)$ (which we approximate as a constants) of order 100.²

The mean flux for loops active at a redshift of z is:

$$\langle \Phi \rangle = \frac{1}{z_f(z) - z} \int_z^{z_f(z)} dz' (1+z')^{-p-1/2} B_0 \lambda_0^2 \quad (2.24)$$

$$= \frac{1}{z_f(z) - z} (-p+1/2)^{-1} B_0 \lambda_0^2 \left[(1+z')^{-p+1/2} \Big|_z^{z_f(z)} \right] \quad (2.25)$$

²One can consider a more detailed model of magnetic field histories but we feel these approximations are sufficient to see the range of possibilities for cosmic ray production.

Using $z_f(z) \approx (\kappa_1)^{-2/3}(1+z)$, we find to a good approximation:

$$\langle \Phi \rangle \approx \frac{B_0 \lambda_0^2}{-p+1/2} (1+z)^{-p-1/2} \kappa_1^{(2p+1)/3} \quad p < 1/2 \quad (2.26)$$

$$\approx \frac{B_0 \lambda_0^2}{p-1/2} (1+z)^{-p-1/2} \kappa_1^{2/3} \quad p > 1/2 \quad (2.27)$$

In particular, for $z = 0$ we see that a recent epoch assumption for the B-field of $p \simeq 1$ gives a mean flux of $\langle \Phi \rangle \approx 10^{39} \text{ gauss cm}^2$ and thus a saturation length $L_s \simeq 10^{20} \text{ cm} (10^{15} \text{ Gev}/M_F)$, while the $p = -1/2$ scenario gives $\langle \Phi \rangle \approx 10^{42} \text{ gauss cm}^2$ and a saturation length $L_s \simeq 10^{23} \text{ cm} (10^{15} \text{ Gev}/M_F)$.

III. Production and Evolution of Cosmic Rays

Given the rate density for the production of superheavy fermions as described in the preceding section we can estimate the resulting cosmic ray spectrum. Here we will assume that each heavy fermion undergoes threebody decays into $n \leq 3$ quarks (we will not distinguish between quarks and gluons in our fragmentation distributions) and $3-n$ leptons. We begin with a discussion of the fate of the hadronic component.

A. Hadronic Component

Quarks or gluons undergo fragmentation into mostly pions and some baryons. The fragmentation distribution cannot be calculated from first principles but Mueller[9] has studied its zeroth moment. Using this and demanding that the first moment be unity (energy conservation) and assuming a convenient $(1-x)^2$ behavior as $x \rightarrow 1$ (of course in QCD the $x \rightarrow 1$ behavior is calculable and energy dependent and *not* of the form $(1-x)^2$ but we are not interested in this limit of the spectrum since the observed cosmic rays extend to $\approx 10^{11} \text{ Gev}$ and the characteristic mass scale of the fermions extends to of order $M_F \approx v \approx 10^{15} \text{ Gev}$; the low- x limit is more relevant to us), we arrive at the following fragmentation distribution[10]:

$$\frac{dN}{dx} = N(b) \exp\left(b\sqrt{\ln(1/x)}\right) (1-x)^2 / (x\sqrt{\ln(1/x)}) \quad (3.1)$$

where:

$$N(b) = \frac{1}{2} \left[e^{b^2/4} I(b) - \sqrt{2} e^{b^2/8} I(b/\sqrt{2}) + \frac{1}{\sqrt{3}} e^{b^2/12} I(b/\sqrt{3}) \right] \quad (3.2)$$

and:

$$I(b) = \frac{\sqrt{\pi}}{2} [\text{erf}(b/2) + 1] \quad b = 4\sqrt{3}/\sqrt{b_o} \quad b_o = 11 - \frac{2n_f}{3} \quad (3.3)$$

We have for $n_f = 6$ that $b \approx 2.6$ and $N(b) \approx .08$. This distribution is engineered so that the zeroth moment obtained in ref.(9) emerges when eq.(3.1) is integrated for a jet of energy E from $x = \mu/E$ to $x = 1$ and μ is chosen of order 1 Gev. For comparison a simple multiplicity growth of \sqrt{E} follows from the distribution:

$$\frac{dN}{dx} = \frac{15}{16} x^{-3/2} (1-x)^2 \quad (3.4)$$

again intergrating from $x = \mu/E$ to $x = 1$. These distributions are displayed in Fig.(1).

Our hadronic injection spectrum at redshift z is then

$$\frac{dN}{dE} \propto f_B \left(\frac{dN}{dx} \Big|_{x=E/M_f} \right) \quad (3.5)$$

where M_f is the heavy fermion mass. Here f_B is unity for pions and is approximately .03 baryons and antibaryons. The pion component induces a neutrino component and we consider this further below. We assume that all baryons ultimately end up as protons though half are initially neutrons which can travel large distances unaffected by magnetic fields at production until they beta-decay to protons, electrons and very low energy neutrinos. Thus, we have a mechanism for injecting extremely energetic nucleons up to energies of order M_f . These will be, in principle, detectable as ultra-high energy cosmic rays, but must be evolved to $z = 0$.

We now must follow the proton cosmic ray spectrum as it undergoes principally three evolutionary effects: (a) cosmological redshift, (b) pion photoproduction, and (c) Bethe-Heitler processes; all other processes are subleading effects [5]. These have been studied in great detail previously [5], but we take several justifiable short-cuts in the present analysis. The redshift effects are straightforwardly included and involve identifying the production energy E_0 at redshift z_0 with an "observer" energy E' at any other redshift z' , $(1+z_0)E' = (1+z')E_0$ (we will be concerned only

with nucleons for which $E > 1\text{TeV}$, and hence are ultra-relativistic) and dilution of the number density by $(1+z)^{-3}$. This latter effect is dominant for a spectrum as flat as that produced at injection by eq.(3.1); we see below that unless the injection spectrum is *increasing* with redshift faster than $(1+z)^4$ that we are sensitive only to the $z \rightarrow 0$ spectrum. Furthermore, there is a gradual energy loss due to e^+e^- production (Bethe-Heitler) which we can include in principle following Blumenthal [12] and ref[5]. In practice, however this effect is negligible on the scale of sensitivity we are presently interested in.

A nucleon colliding with a microwave background photon is above threshold to undergo photoproduction of pions if $E > 2m_\pi^2/((1+z)T_{30K})$. The recoil nucleon at extremely high energies is approximately uniformly distributed in energy between incident and threshold energy and will be neglected in the present analysis (see ref.[5] for a discussion of the relevant corrections). This implies that there will be a Greisen cut-off to the high energy cosmic ray spectrum if the source of cosmic rays is greater than a few interaction lengths (one energy loss length is about 6 Mpc today) away [11].

An interesting signature for superconducting strings emerges in this analysis. If there are active strings within a few interactions lengths then there will be no complete Greisen cut-off, but rather a dip in the spectrum will occur above the cut-off, extending to very high energies, and super-ultra-high energy cosmic rays will be seen at energies above the upper limit of the dip.

To see this effect, consider a single cosmic string of total luminosity, L_0 , at sufficient range to be considered a point source. For definiteness take the particle production rate of the preceding section :

$$L_0 \approx 2g^3 v \gamma_{em} \alpha' \alpha = 2\gamma_{em} \alpha' \alpha M_F^3 / v^2 \quad (3.6)$$

We see the very strong dependence upon M_F in the activity (there is further dependence through the fragmentation spectrum). The observed differential energy flux at range R for nucleons, including the Greisen cut-off (but neglecting redshift effects) becomes:

$$j(E) \approx \frac{f_B n L_0}{4\pi R^2 M_F} \left(\frac{dN}{dx} \Big|_{x \rightarrow E/M_f} \right) e^{-R/\lambda(E)} \quad (3.7)$$

Here we neglect pile-up effects and a suitable parameterization for $\lambda(E)$ may be taken from [13]. $\lambda(E)$ has weak energy dependence above threshold and is about 6Mpc over the decade in energies above 10^{20} eV.

In Figure(2) we give the resulting fluxes at earth for various ranges of the single point source assuming $M_F = 10^{16}$ Gev, out to $R \sim 100$ Mpc at which point this simple $z \sim 0$ approximation begins to break down. For comparison we plot a $1/E^3$ spectrum with the approximate normalization observed at the Fly's Eye [15] for hadronic UHE cosmic rays up to 10^{20} eV. We extrapolate the Fly's Eye normalization for a *fixed number of events* above 10^{20} ev, i.e. a limiting line going as $\approx E^2$.

For the assumed value of the source luminosity we can barely tolerate a single distant point source at range $R \approx 30$ Mpc. Of course, as we see subsequently, by reducing M_F we can have a tolerable contribution to the spectrum.

We turn now to a more detailed analysis of source vs. red-shift distributions. Our procedure for treating the collisional and red-shift effects is much simpler than that employed in [5] but is reasonably faithful to most of the gross effects. We do not treat the thermal fluctuations in target photon energy and the detailed evolution dynamics have been considerably simplified by approximate recoil distributions.

We will assume the rate densities are determined as in Section II.C. Thus, the source activity density is given by:

$$j(E, z) = \frac{dn(z)}{dL} L_s \dot{N}(z) \frac{1}{M_F} \left(f_B \frac{dN}{dx} \Big|_{x \rightarrow E/M_f} \right) \quad (3.8)$$

and using the results for these quantities as obtained in Section II we have:

$$j(E, z) = \frac{\gamma_{em} H_0^4 \alpha' \alpha}{\kappa_1^2} \left(\frac{\pi f_{\Phi} M_F^2 \langle \Phi \rangle_x}{2eg \log(L/2\pi l)} \right) (1+z)^6 \left(f_B \frac{dN}{dx} \Big|_{x \rightarrow E/M_f} \right) \quad (3.9)$$

The flux measured at Earth requires integrating over radial cosmic coordinates $r(z)$ and is given by:

$$J(E, z) = \int_0^\infty \frac{j(E/(1+z), z(r)) R(t_r)^3 r^2 dr}{R(t_0)^2 r^2} e^{-r/\Lambda'(E/(1+z))} \quad (3.10)$$

$$= \int_0^\infty \frac{j(E/(1+z), z)(1+z)^{-4} dz}{(1+z)^{1/2} H_0} e^{-r(z)/\Lambda'(E/(1+z))} \quad (3.11)$$

where $\Lambda'(E)$ depends upon redshifted energy (Recall that we consider an $\Omega = 1$ Universe so that $k = 0$ and $q_0 = 1/2$). We find then using the approximate expressions for the flux as given in eq.(2.26) that the spectrum for $p < 1/2$ is:

$$J(E, z) \approx \frac{\pi\gamma_{em}\alpha\alpha'g^2H_0^3f_Bf_{\Phi}B_0\lambda_0^2}{M_F\kappa_1^2(1-2p)e\log(L/2\pi l)}\left(\frac{\kappa_1}{c}\right)^{(1+2p)/3} \int_0^\infty dz(1+z)^{1-p}\theta(E_c/(1+z)-E)\left(\frac{dN}{dx}\Big|_{x\rightarrow E/(1+z)M_f}\right) \quad (3.12)$$

where $\theta(E_c/(1+z)-E)$ ($\theta(x)$ is the ordinary step function) approximates the large redshift cut-off effects [5]. There is an analogous expression corresponding to the magnetic evolution $p > 1/2$ using eq.(2.27). In practice, we must evaluate these numerically. We find no significant differences between the simple distribution, eq.(3.4) and that of eq.(3.1).

In Figure (3) we present the results for the evolved injection spectra following various assumptions about the primordial B-field as parameterized by p and a fermion mass equal to 10^{15} Gev. We see that negative p can be ruled out, and that $p > 0$ scenarios contain the possibility of a dip extending to very high energies. Here the dashed line is defined by the Fly's Eye normalization of the UHE spectrum [15] and which has been extrapolated above 10^{20} ev by assuming a constant (with energy) integrated spectrum with normalization fixed by the limit at 10^{20} ev produces the same likelihood of a recorded event per unit time.

In Figures (4) and (5) we consider the light fermion masses of 10^{13} Gev and 10^{11} Gev respectively. We see that a light fermion of 10^{11} Gev is minimally compatible with OTW and cannot be ruled out. These cases *may in fact account in part for the observed UHE cosmic rays.*

B. The Neutrino Spectrum

Presently we consider the neutrinos which may emerge from: (a) direct decay products of the massive fermion ejected from the string, (b) fragmentation products from the decays of pions in the quark jets, and (c) induced neutrinos from the proton collisions with microwave photons in transit to detector [5, 6].

Neutrinos produced by mechanism (a) constitute approximately a flat energy distribution at injection (boosted β -decay distribution):

$$\frac{dN_\nu}{dE} \simeq \frac{3}{M_F} \theta(M_F/3 - E(1+z)) \quad (3.13)$$

where E is the energy at detection. In mechanism (b), each muon neutrino produced in charged pion decay has a flat energy (x) distribution up to the pion energy. Upon convoluting the quark fragmentation distribution with this flat spectrum we obtain:

$$\frac{dN_\nu}{dE_\nu} = \int \theta(x-x_\nu) \frac{1}{x} \frac{dN_\pi}{dx} dx \Big|_{x \rightarrow E/M_f} = \frac{15}{16} \left(\frac{16}{3} - \frac{6x_\nu^2 + 12x_\nu - 2}{3x_\nu^{3/2}} \right) \Big|_{x \rightarrow E/M_f} \quad (3.14)$$

where the pions, for simplicity, have been described by the quark fragmentation distribution of eq.(3.4) For mechanism (c), the neutrinos produced by the decays of secondary pions in $N + \gamma \rightarrow \pi + N'$ are determined by the nucleon spectrum above the Greisen cut-off energy. If we let $x = 1$ correspond to the maximum energy and x_c the Greisen cut-off energy, these neutrinos have energy distributions with essentially the form of eq.(3.14) for $x > x_c$ and is flat for $x < x_c$. In normalizing this contribution we must include the multiplier effect due to the fact that the recoil nucleon, N' does not drop immediately below threshold and the fact that the average number of successive photoproduction reactions per nucleon is roughly $0.3 \log(x/x_c)$.

These three contributions to the neutrino spectrum are shown in Figure(6). By far, the multiplicity is dominated by the pion decays in a quark jet. In Figure (7) we present the results for the evolved neutrino spectra following various assumptions about the primordial B-field as parameterized by p . We assume here that the fermion mass is equal to 10^{15} Gev . We see that all $p < -1$ can be ruled out. Here the dashed line is defined by the Fly's Eye limit on deeply penetrating particles [15] using total neutrino cross-sections of ref.[14], and which has been extrapolated above 10^{20} ev by assuming a constant (with energy) integrated spectrum with normalization fixed by the limit at 10^{20} ev produces the same likelihood of a recorded event per unit time. Remarkably, the limit on the neutrino spectrum is somewhat more constraining than that of the nucleon spectrum, a consequence of the larger number of neutrinos per heavy fermion decay than baryons and the lack of a Greisen cut-off.

In Figures (8) and (9) we consider the light fermion masses of 10^{13} Gev and 10^{11} Gev respectively. Once again we see that a light fermion of 10^{11} Gev is minimally compatible with OTW and cannot be ruled out.

IV. Summary and Conclusions

In this work we have discussed the production of ultra-high energy cosmic rays by superconducting loops of cosmic string. We assume that the superconducting cosmic strings have size distributions as a function of redshift and mass per unit length so that they are consistent with galaxy formation scenarios. A general parameterization of the magnetic flux history of these loops then allows one to calculate the production of massive fermion pairs from saturated loops and to follow the evolution of the high-energy cosmic rays produced by their decay. Our calculations may be summarized as follows:

1. An active loop of superconducting cosmic string within 30 Mpc, which decays into fermions with masses of the order of the vev of the broken U(1) which produced the string ($\approx 10^{15} \text{Gev}$), would generate observable cosmic rays above the Greisen cut-off ($\approx 10^{20} \text{eV}$). While this prediction is independent of the magnetic field history of the loop (although the density of such objects in the Universe is), the critical range outside which such a loop could not be “seen” can be tuned by an appropriate choice of fermion mass.
2. The evolved cosmic ray spectrum which results from the contributions of large-redshift active superconducting cosmic strings can be made consistent with the observed ultra-high energy cosmic rays by tuning the fermion mass and/or the evolution of magnetic fields. In fact, if we assume a magnetic field energy density which scales as the radiation density to a value of $\approx 10^{-7} \text{gauss}$ today, then our calculations indicate that the cosmic rays produced by evaporating superconducting cosmic strings could be responsible for all of the observed ultra-high energy cosmic rays.

In both cases, decreasing the fermion mass or requiring that intergalactic magnetic fields are produced during a recent epoch will reduce the resultant flux of cosmic rays. It is striking that UHE cosmic ray physics places such limits upon a hypothetical microphysical process and conversely that such fundamental processes may be observable by large scale cosmic ray detectors.

Acknowledgements

We are grateful to Rich Holman for useful discussions.

References

1. J. P. Ostriker, C. Thompson, E. Witten, *Cosmological Effects of Superconducting Strings*, Princeton Preprint (1986)
2. E. Witten, *Nucl. Phys.* **B249**, 557 (1985)
3. B. Paczynski and D. Spergel, Princeton Observatory Preprint-182.
4. A. Albrecht, N. Turok, *Phys.Rev.Lett.* (*in press*)
5. C. T. Hill, D. N. Schramm, *Phys. Rev.* D31, 564 (1985), *Phys. Letters* **131B**, 247 (1983), and refs. therein.
6. C.T. Hill, D.N. Schramm, T.P. Walker, *Phys.Rev.*,D**34**, 1622 (1986)
7. A. Vilenkin, *Physics Reports*, **121**, 263 (1985)
8. Y. Rephaeli, M. Turner, *Phys.Lett.*, 121B, 115 (1983).
9. A. H. Mueller, *Phys. Letters* **104B**, 161 (1981)
10. C. T. Hill, *Nucl. Phys.* **B224**, 469 (1983).
11. K. Greisen, *Phys.Rev.Lett.* **16**, 748 (1966); G.T. Zatsepin, V.A. Kuz'min, *Pis'ma Zh. Eksp. Teor. Fiz.* **4**, 114 (1966).
12. G. Blumenthal, *Phys.Rev.* **D 1**, 1596 (1970)
13. M. Giler, J. Wdowczyk, A. Wolfendale, *J. Phys. G* **6**, 1561 (1980); A. Strong, J. Wdowczek, A. Wolfendale, *J. Phys. A* **7**, 120 (1974) and **A 7**, 1767 (1974)
14. C. Quigg, M.H. Reno, T.P. Walker, *Phys.Rev.Lett.*, 57, 774 (1986)

15. R.M. Baltrusaitis, R. Cady, G.L. Cassiday, R. Cooper, J.W. Elbert, P.R. Gerhardy, S. Ko, E.C. Loh, Y. Mizumoto, M. Salamon, P. Sokolsky, D. Steck, Print-85-0305 (UTAH), and Phys.Rev.,**D31**, 2192 (1985), and Phys. Rev. Lett., **54**, 1875 (1985)

Figure Captions

1. The x-distributions assumed for quark fragmentation (A) eq.(3.1 (B) eq.(3.4); and the corresponding nucleon spectra, (C) and (D), assuming 3% nucleons plus antinucleons per total multiplicity.
2. The UHE nucleon spectrum for a point source at distances (A) 3 Mpc; (B) 10 Mpc; (C) 30 Mpc; (D) 100 Mpc in the approximation of neglecting redshift effects. We assume $\alpha = 1/137$, $\alpha' = 1/40$, $\gamma_{em} = 100$ and $M_F = 10^{15} \text{ Gev}$ ($g = 1$). We've superimposed the "QCD" results with eq.(3.1) (solid) upon eq.(3.4) (dots) to indicate that they are nearly indiscernible. The horizontal line (dot-dashed) represents the Fly's Eye's normalization of the differential spectrum extrapolated up to 10^{20} ev . Above 10^{20} ev we assume a limit determined by a fixed number of events in a given period of time (equivalent to a constant integrated spectrum, independent of energy).
3. The UHE nucleon spectrum integrated over redshift for $M_F = 10^{15} \text{ Gev}$ and all other parameters as in Fig.(2)
4. The UHE nucleon spectrum integrated over redshift for $M_F = 10^{13} \text{ Gev}$ and all other parameters as in Fig.(2)
5. The UHE nucleon spectrum integrated over redshift for the indicated magnetic flux-history parameterization, p. We assume here the minimal $M_F = 10^{11} \text{ Gev}$ and all other parameters as in Fig.(2)
6. The x-distribution of produced neutrinos due to (A) quark fragmentation pion decays; (B) secondary pion decays in $N + \gamma(3^0K) \rightarrow \pi + N'$ assuming $x_c = 10^{-4}$; (C) direct neutrinos from heavy fermion decay. Note that $x = 1$ correspond to maximum energy $\approx M_F/3$ in three body decays.

7. The UHE neutrino spectrum integrated over redshift for $M_F = 10^{15}$ *GeV* and all other parameters as in Fig.(2)
8. The UHE neutrino spectrum integrated over redshift for $M_F = 10^{13}$ *GeV* and all other parameters as in Fig.(2)
9. The UHE neutrino spectrum integrated over redshift for the indicated magnetic flux-history parameterization, p. We assume here the minimal $M_F = 10^{11}$ *GeV* and all other parameters as in Fig.(2)

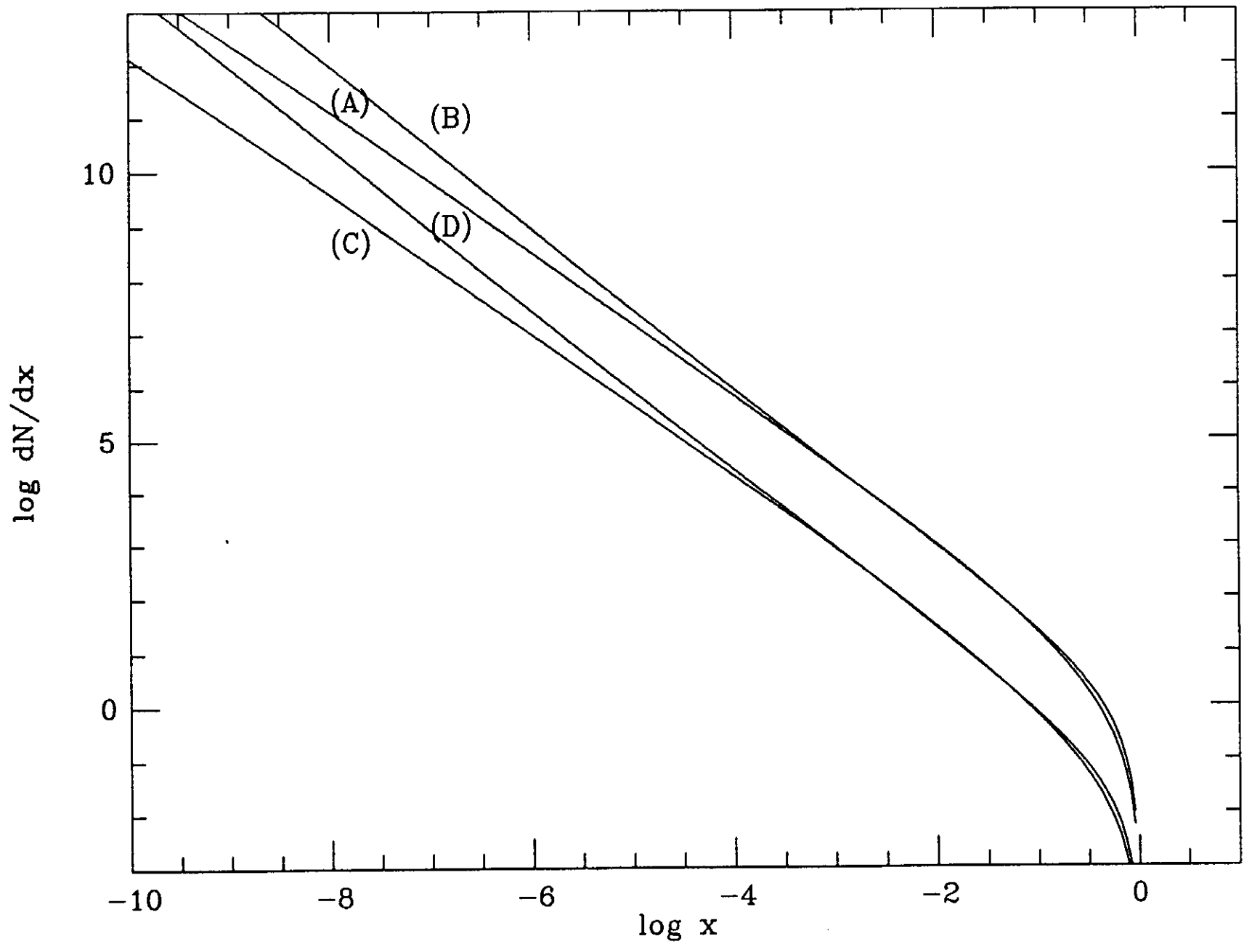


Figure 1

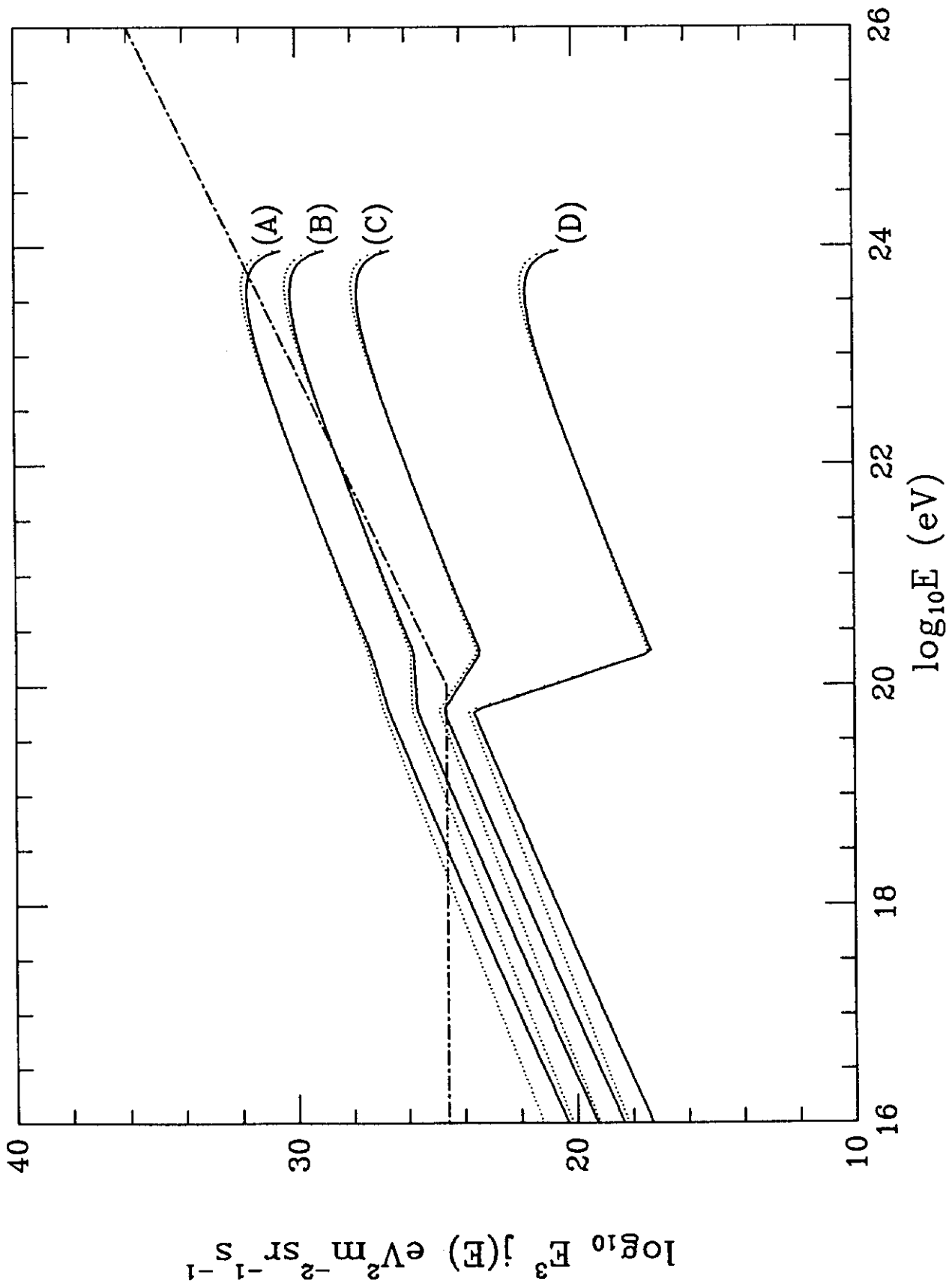


Figure 2

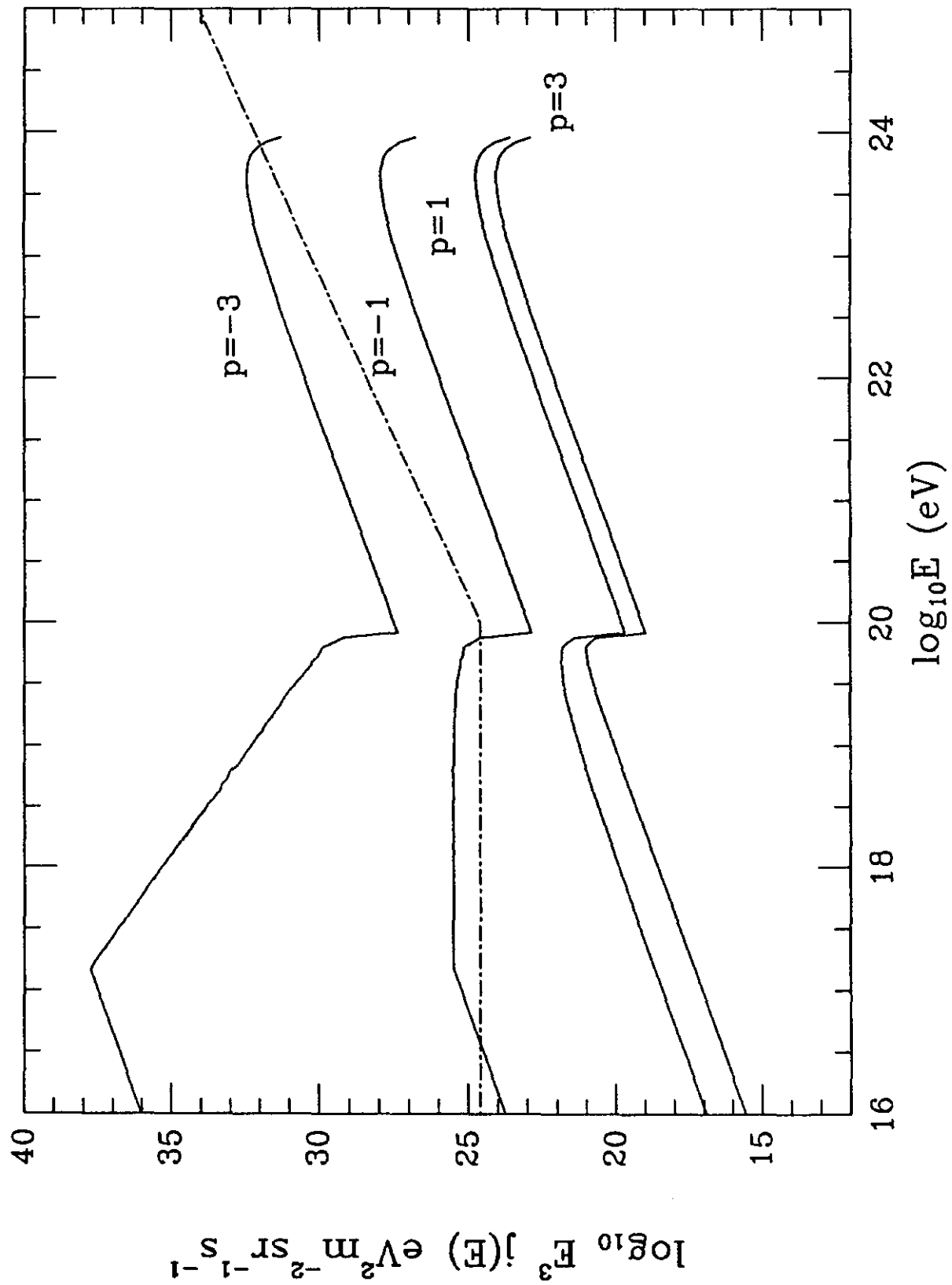


Figure 3

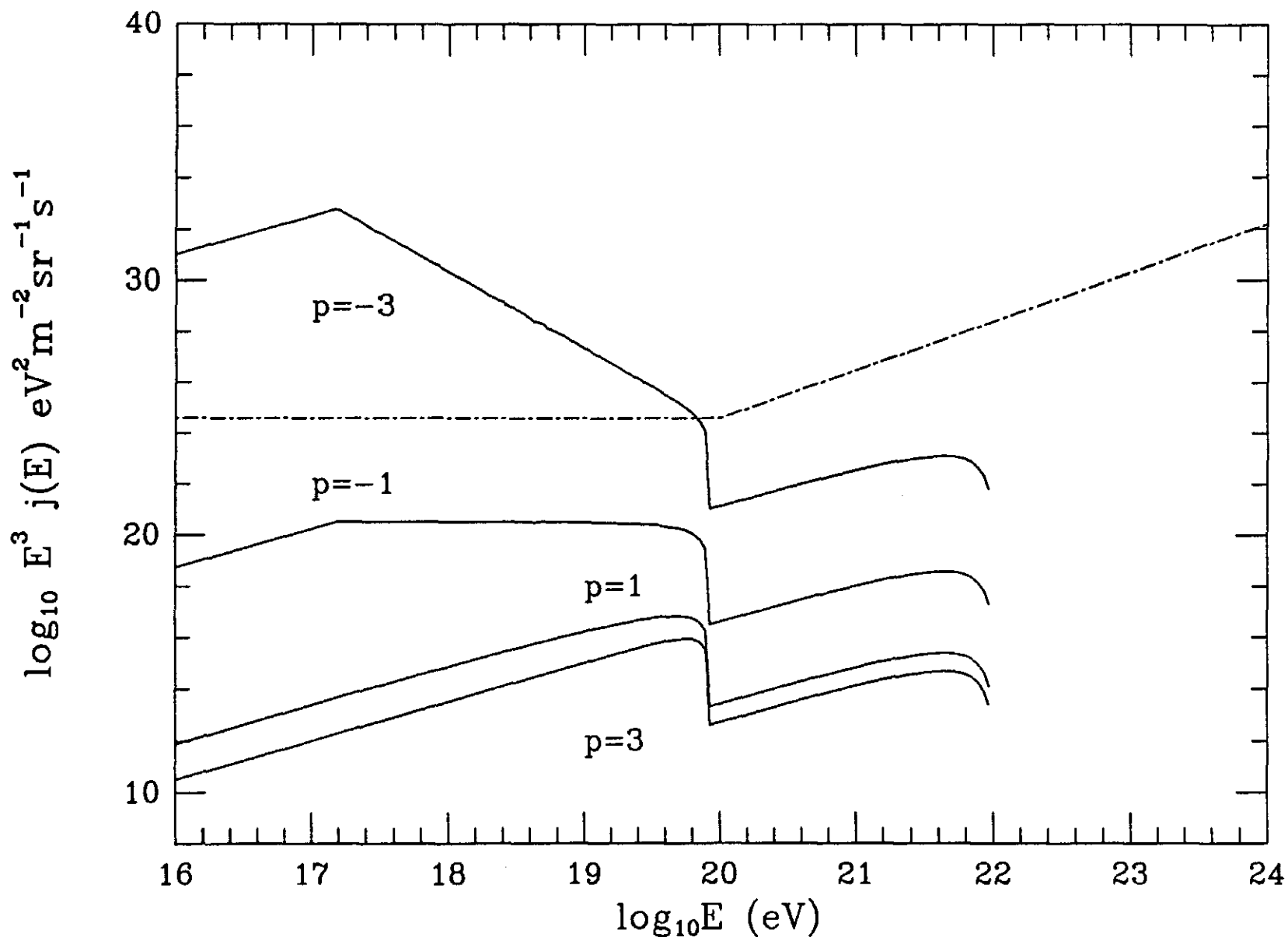


Figure 4

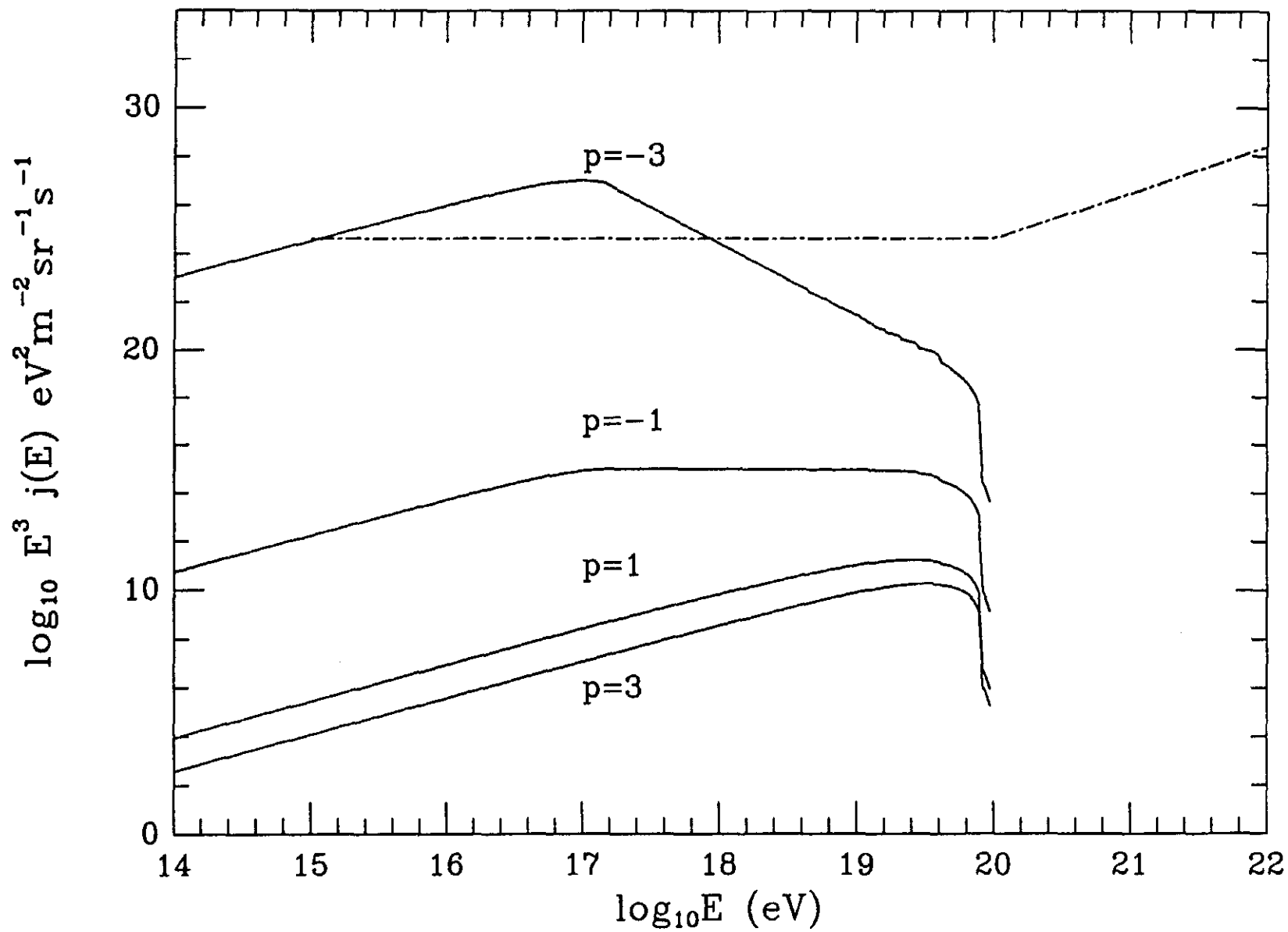


Figure 5

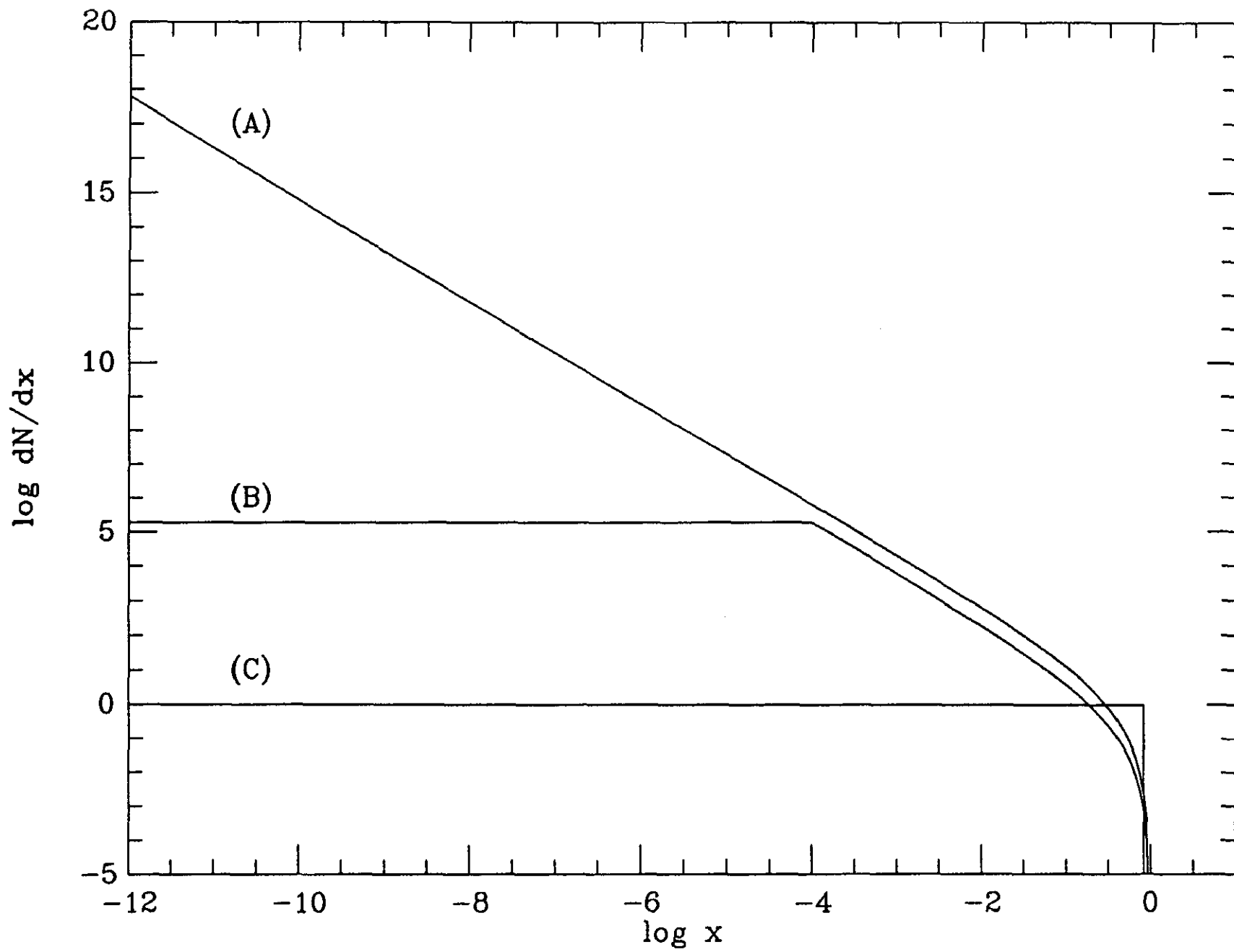


Figure 6

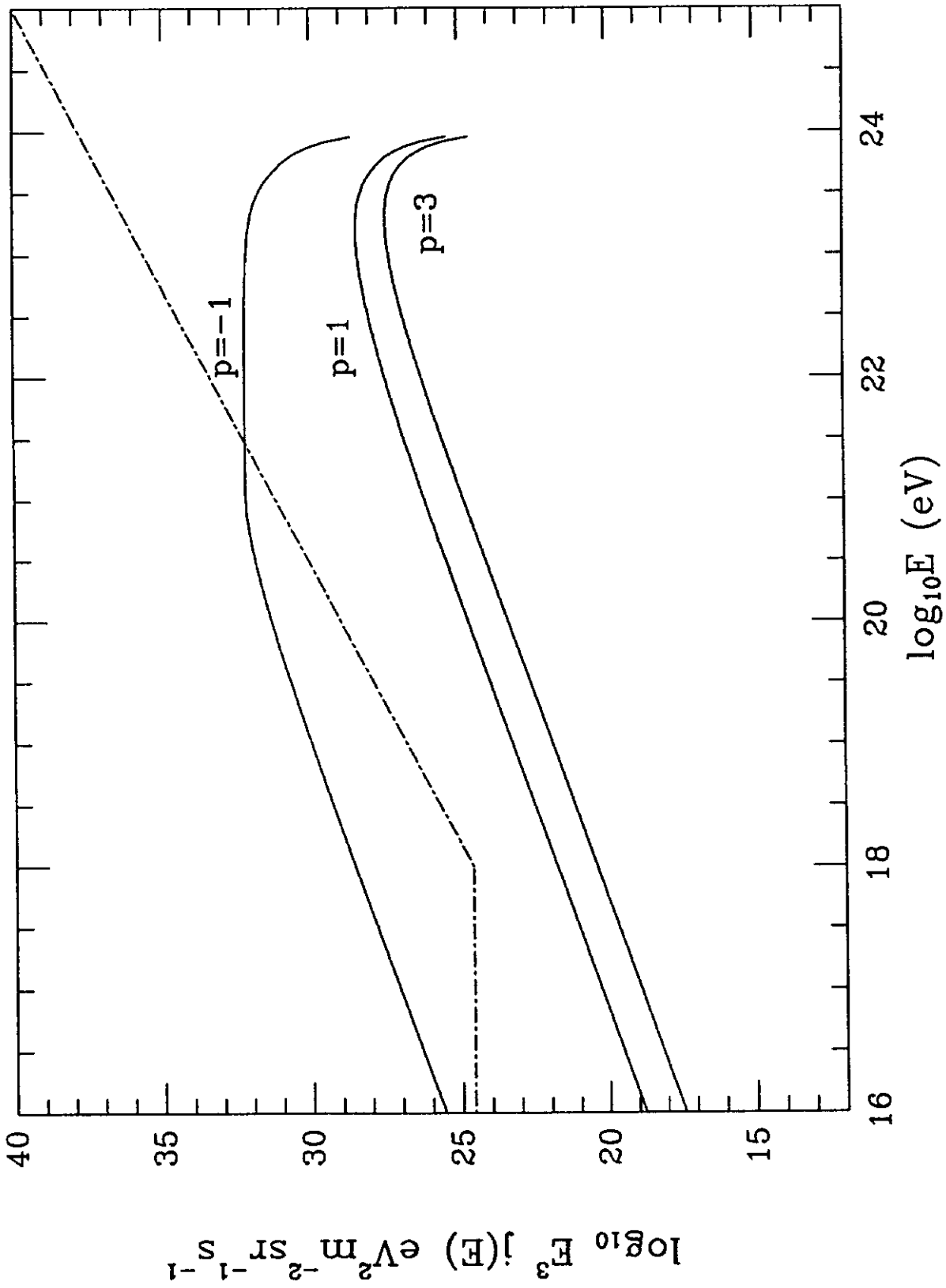


Figure 7

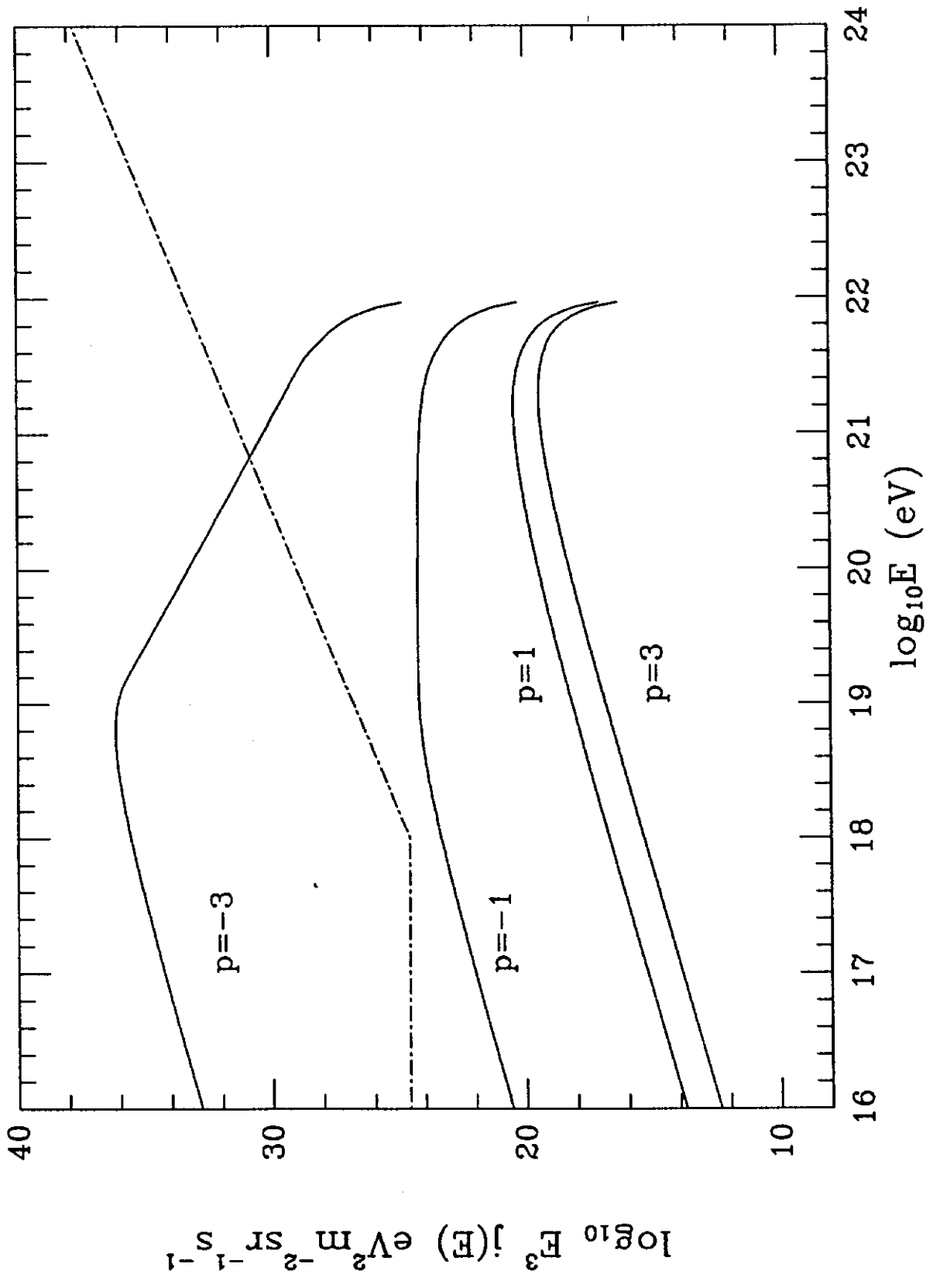


Figure 8

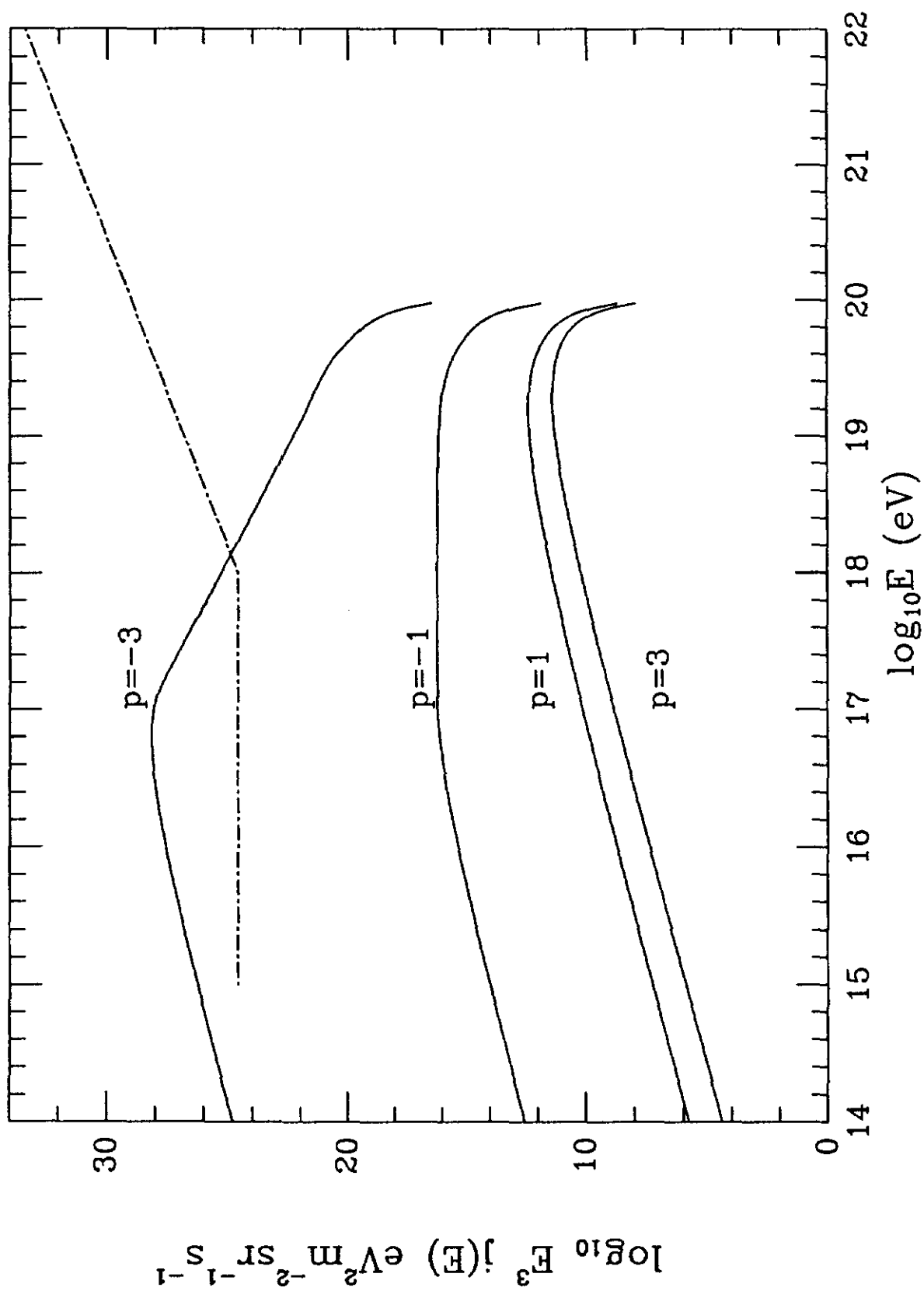


Figure 9